# Predictions of seismic velocity models (time and depth) by combining diffraction filter and residual diffraction moveout

J.A.C. Gonzalez (Faculty of Geophysics-UFPA), J. Jadsom Sampaio de Figueiredo* (INCT-GP & Faculty of Geophysics-UFPA), T.A. Coimbra (CEPETRO-University of Campinas -UNICAMP), J. Schleicher (University of Campinas - UNICAMP & INCT-GP) and A. Novais (University of Campinas-UNICAMP & INCT-GP)

Copyright 2015, SBGf - Sociedade Brasileira de Geofísica

This paper was prepared for presentation at the International Congress of the Brazilian Geophysical Society, held in Rio de Janiero, Brazil, August 3-5 2015.

Contents of this paper were reviewed by the Technical Committee of the 14th International Congress of The Brazilian Geophysical Society and do not necessarily represent any position of the SBGf, its officers or members. Electronic reproduction or storage of any part of this paper for commercial purposes without the written consent of The Brazilian Geophysical Society is prohibited.

## Abstract

**In this work, we develop a practical approach to construct velocity models in the time and depth domains using seismic diffractions. This methodology applies plane wave destruction (PWD) filters jointly with the residual diffraction moveout (RDM) method. Its only requirements are the presence of identifiable diffraction events after filtering out the reflection events and an arbitrary initial velocity model as input. We compare post-stack migrated images (in the time and depth domains) with images migrated with models obtained from conventional seismic processing. In both cases, we used post-stack Kirchhoff migration. Beyond the need to identify and select the diffraction events in the post-stack migrated sections in the depth domain, the method has a very low computational cost. The processing time to reach an acceptable velocity model was 75 % less as compared with conventional processing. The applicability of our methodology was verified using a real Viking Graben seismic dataset.**

## Introduction

It is well known that when seismic waves interact with small structures in the subsurface of the earth (e.g., faults, fractures, channels, and rough edges of salt bodies), waves are scattered in all directions. The typical scattered signatures, known as diffractions, have been investigated for a long time with the purpose of understanding their signatures and how they could be used in seismic processing. Adequate usage of diffraction information in routine practice can be helpful in interpreting hydrocarbon traps in the subsurface and their final delineation (Tsingas et al., 2011). Special features exhibited by diffraction signatures (hyperbolae) have been particularly useful in the application of diffractions in velocity analysis (Sava et al., 2005; Novais et al., 2008; Landa and Reshef, 2009; Coimbra et al., 2013), super-resolution (Khaidukov et al., 2004), linear fracture imaging (Alonaizi et al., 2013) and $CO_2$ time-lapse monitoring (Alonaizi et al., 2014).

Reflections and diffractions are two types of coherent events generated in the subsurface. However, in conventional processing, most time is spent on reflections, while diffractions are considered noise due to their weak seismic energy. Particularly, conventional processing distorts the shape of a diffraction. Therefore, the true information about the structure contained in this kind of event (Zhang, 2009) is lost most of the time. Therefore, it is desirable to separate the reflected energy from the diffractions before carrying out the analysis of the latter.

For this reason, a number of recent studies have concentrated on separating diffractions from reflections. Khaidukov et al. (2004) proposed to mute the reflections by focusing and defocusing the residual wavefield in a shot gather that contains mostly shot diffractions. Klokov and Fomel (2013) used the Radon transform to separate diffractions from reflections in the dip-angle domain. Liu et al. (2013) proposed the singular-spectrum-analysis (SSA) method, which removes diffractions from the full wavefield by taking advantage of the difference between the kinematic and dynamic properties of reflections and diffractions (Landa et al., 1987; de Figueiredo et al., 2013).

Once the reflections have been filtered out, the diffracted energy is more accessible to further processing. In this work, we have implemented a diffraction filter based on plane-wave-destruction (PWD) filters (Claerbout, 1992; Fomel, 2009) with the local-slope correction developed by Schleicher et al. (2009). This correction is based on the fact that the slope's inverse can be extracted from the data in a fully analogous way to the slope itself. Combining the information of the slope and its inverse yields a simple but effective correction to the local slope. In our implementation of the PWD filters, we smooth over the so-extracted local slopes. Other slope-extraction methods are discussed in Hale (2007).

After filtering out the reflections, we then performed a velocity analysis on seismic diffraction panels. Our velocity analysis was based on the residual-diffraction-moveout (RDM) technique developed by Coimbra et al. (2013). The method was originally developed for zero-offset data. Here, we apply it to a stacked section and a near-offset section. The error resulting from the applying the method to a non-zero offset section is overcome after very few iterations. The number of necessary iterations depends on the complexity of the dataset. Finally, we compare the migrated seismic images (in the time and depth domains) obtained by conventional seismic processing with those obtained by the our processing sequence using RDM velocity analysis (which we will refer to as RDM processing). An application of RDM processing to a real Viking Graben seismic dataset confirms the applicability of our method.

**Methodology**

In this section, we describe our methodology for the analysis based on residual-diffraction-moveout (RDM) processing. The corresponding processing sequence makes use of plane-wave-destruction (PWD) filters to separate diffractions from reflections in near-offset sections before RDM velocity analysis. After the separation, the method uses the residual moveout of incorrectly migrated diffraction events in depth domain to update the velocity model. Although the theory is developed for zero-offset sections, we started the procedure with a near-offset section and used a normal-moveout (NMO) stacked section in the next iteration. The resulting error is negligible after very few iterations.

*PWD filter and local slope*

The RDM method uses the information carried by incorrectly migrated diffractions to determine updates for the velocity model. However, it is well known that reflection energy is dominant over diffraction energy. Therefore, it is necessary to separate or attenuate the reflections against the diffractions, if we want to use diffractions in seismic processing. According to Claerbout (1992), a plane-wave destruction (PWD) filter can be used to attenuate the nearly planar events associated with reflections. Such a PWD filter can be defined by means of the local plane-wave differential equation given by

$$\frac{\partial P}{\partial x} + \sigma \frac{\partial P}{\partial t} = 0, \tag{1}$$

where $P$ is the wavefront that depends on offset $x$, time $t$, and the local-slope parameter $\sigma$. To implement a PWD filter according to equation eq:10, we need an estimate of $\sigma$. Then, by considering only a slowly varying background slope field, we can filter out the events with an almost constant slope, which are most likely reflections, and preserve events with stronger slope variations, which will include diffractions.

To determine the local slope $\sigma$ at a point $(x_i, t_j)$ in the data section, Claerbout (1992) suggested to use an iterative method to find the data residual, i.e., those parts of the data that do not satisfy equation eq:10. This residual is given by

$$R(\sigma) = \sum_{i,j}^{W} \left( \frac{\partial P(x_i,t_j)}{\partial x} + \sigma \frac{\partial P(x_i,t_j)}{\partial t} \right)^2, \tag{2}$$

where $W$ is the size of windows selected around of the point $(x_i, t_j)$. Fomel (2009) implemented an all-pass filter to find a similar solution using a finite-difference approximation of equation eq:10 in the frequency domain, although this process required high computational resources. For this reason, we used the simpler method of Schleicher et al. (2009) to estimate $\sigma$ and the quadratic residual $R(\sigma)$.

The idea of the work of Schleicher et al. (2009) is to apply the original procedure of Claerbout (1992) twice. For the second application, they rewrite equation 1 as

$$q \frac{\partial P}{\partial x} + \frac{\partial P}{\partial t} = 0, \tag{3}$$

where $q = 1/\sigma$. Then, in correspondence to the technique of Claerbout (1992), the quadratic residual is given by

$$R(q) = \sum_{i,j}^{W} \left( q \frac{\partial P(x_i,t_j)}{\partial x} + \frac{\partial P(x_i,t_j)}{\partial t} \right)^2. \tag{4}$$

The results of equations 2 and 4 can be combined to provide a simple and effective correction of the local-slope measure. According to Schleicher et al. (2009), the least-squares value of $\sigma$ is given by

$$\langle \sigma \rangle_E = S \left( \sqrt{\frac{\sum_{i,j}^{W} \left( \frac{\partial P(x_i,t_j)}{\partial x} \right)^2}{\sum_{i,j}^{W} \left( \frac{\partial P(x_i,t_j)}{\partial t} \right)^2}} \right), \tag{5}$$

where $S$ is defined as

$$S = -\left( \sum_{i,j}^{W} \left( \frac{\partial P(x_i,t_j)}{\partial x} \right) \left( \frac{\partial P(x_i,t_j)}{\partial t} \right) \right). \tag{6}$$

Equation eq:13 minimizes the error of the least-squares solution of both equations eq:11 and eq:13 simultaneously. To implement equation eq:10, any method can be used to estimate the slope, as long as a good estimate of this seismic parameter can be obtained. Before applying our RDM processing sequence to real data, we performed several tests of PWD filters on synthetic data. Figure 1a shows the Sigsbee2B dataset used to test our PWD filter. Figure 1b is the local-slope panel estimated and Figure 1c is the diffraction panel after PWD filter application. We can see in Figure 1c that the energy of planar events is reduced and that the energy of diffraction events is more visible. Note that perfect removal of reflected energy is not required by the RDM method. It is only necessary that diffraction events can be identified and interpreted.

*RDM analysis*

Recently, Coimbra et al. (2013) developed a method for diffraction-point imaging and local migration velocity improvement based on the localization and picking of the residual moveout of incorrectly migrated diffraction events in the depth domain. Here, we apply this methodology to construct velocity models in both the depth and time domains. According to Coimbra et al. (2013), considering a diffraction point at the true position $(x_t, z_t)$ in a constant-velocity medium with true velocity $v_t$, the residual moveout of a diffraction event after of depth migration with an incorrect velocity $v_0$ coincides with the Huygens image-wave for the depth remigration from velocity $v_t$ to $v_0$. The location of the Huygen's image-wave is defined as the curve or surface of all points where a possible event of the image point $(x_t, z_t)$ might be placed when the migration velocity is changed from $v_t$ to $v_0$ (Hubral et al., 1996). As a consequence, if the migration velocity is higher than the true medium velocity, an overmigrated diffraction event will have shape of an ellipse or if the migration velocity is smaller, the shape of an undermigrated diffraction event is a hyperbola. Mathematically, the resulting curve is given by (Hubral et al., 1996)

$$\frac{z^2}{v_0^2} + \frac{(x - x_t)^2}{v_0^2 - v_t^2} = \frac{z_t^2}{v_t^2}. \tag{7}$$

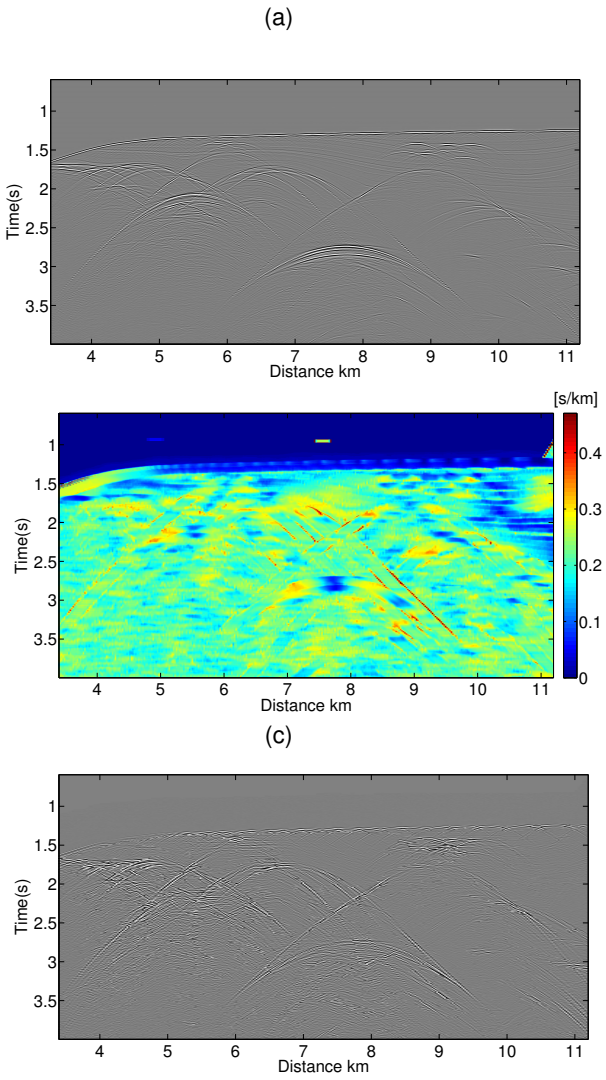


Figure 1: (a) The Sigsbee2B synthetic dataset. (b) Local-slopes panel. (c) Diffraction section PWD filter application.

To emphasize the hyperbolic or elliptic shapes, Coimbra et al. (2013) rewrite equation 7 in the form

$$\frac{z^2}{b^2} + s\frac{(x-x_t)^2}{a^2} = 1, \tag{8}$$

where the half-axes $a$ and $b$ are given by

$$a = \frac{z_t}{v_t}\sqrt{|v_0^2 - v_t^2|} \quad and \quad b = \frac{z_t}{v_t}v_0. \tag{9}$$

Depending on the sign $s = sgn(v_0^2 - v_t^2) = sgn(v_o - v_t)$ equation 8 can represent an ellipse or a hyperbola.

Coimbra et al. (2013) used a least-squares method to find the best-fitting hyperbola or ellipse to describe an incorrectly migrated diffraction event. This provides estimates for the half-axes $a$ and $b$ as well as the horizontal coordinate of the apex $x_t$. Note that the $a$ and $b$ parameter are related to the slope of incorrectly migrated diffraction.

In a medium with a strong velocity gradient, this slope can be quite affected. To allow for stronger velocity gradients, Coimbra et al. (2013) modified equation eq:3 to

$$\frac{z^2}{b^2} + s\frac{(x-x_t)^2}{a^2} = 1 + \varepsilon\,(x-x_t)\,z, \tag{10}$$

where $\varepsilon(x-x_t)z$ is a perturbation term to allow for a rotation of the ellipse or hyperbola. The parameter $\varepsilon$ is adjusted simultaneously with the other parameters of the ellipse or hyperbola in the least-squares procedure, but not used in the velocity-updating procedure.

The residual moveout of the incorrectly migrated diffraction events can then be used to update the migration velocity model. According to Coimbra et al. (2013) there are two ways to update the velocity model. One of them is related to the half-axes and the other one is using remigration trajectories, i.e., the curves connecting all positions where a migrated point can be found for different migration velocities. More details about the RDM method can be found in Coimbra et al. (2013).

Figure 2 shows a pictorial illustration of under- and overmigrated diffraction curves (black lines) with remigration trajectories (red lines). The black lines in Figure 2c and 2d are the hyperbola and the ellipse described by equations 8 and 9.

*RDM processing*

We combined the PWD filtering with the RDM velocity analysis into a new processing sequence for seismic diffractions. The new RDM processing to construct a velocity model, starting from a nearest-offset section, applies the PWD filter to separate diffraction events, and applies the residual diffraction moveout method to obtain a velocity model. The flowchart is depicted in Figure 3. Specifically, RDM processing consists of the following steps:

1. Pre-processing (geometry correction, trace editing, deconvolution, band-pass filtering and AGC) of the (real) dataset. This work was performed for the conventional and RDM processing.

2. Selection of the nearest-offset gather from the real dataset.

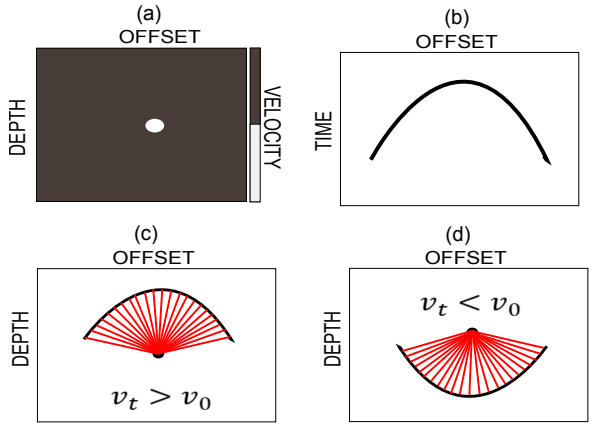


Figure 2: Pictorial illustration of incorrectly migrated diffraction events and remigration trajectories. (a) Constant velocity model with a scattering point located at the center of the model. (b) Zero-offset section over this diffraction point. (c) Remigration trajectories (red line) starting at an undermigrated hyperbolic diffraction curve (black line). (d) Remigration trajectories (red line) starting at an overmigrated elliptic diffraction curve (black line).

3. Calculation of the local slope for each point in the nearest-offset gather.
4. Application of the PWD filter to separate diffractions from reflections in the nearest-offset gather.
5. Migration of filtered diffractions using a constant velocity model with $v = 1500$ m/s.
6. Application of RDM velocity analysis using this migrated gather to find the first velocity model.
7. Application of an NMO stack with the current velocity model to the full dataset to obtain an improved ZO section, input to the next iteration.
8. Calculation of the local slope for each point in the current ZO section.
9. Application of the PWD filter to separate diffractions from reflections in the current ZO section.
10. Migration of filtered diffractions using the current velocity model.
11. Application of RDM velocity analysis on this gather to update the current velocity model.
12. Iteration of steps 7 to 11 until all identifiable diffractions are collapsed.
13. Depth and time migration of the final stacked section with the conventional and RDM velocity models.

In our application of the above processing sequence to a real Viking-Graben dataset, only two iterations of the above procedure (one with the nearest-offset gather, one with the first NMO-stacked section) were necessary to find an acceptable migration-velocity model. Other data may require more than two iterations. It is to be expected that the number of required iterations will depend on the complexity of the data.

(a)

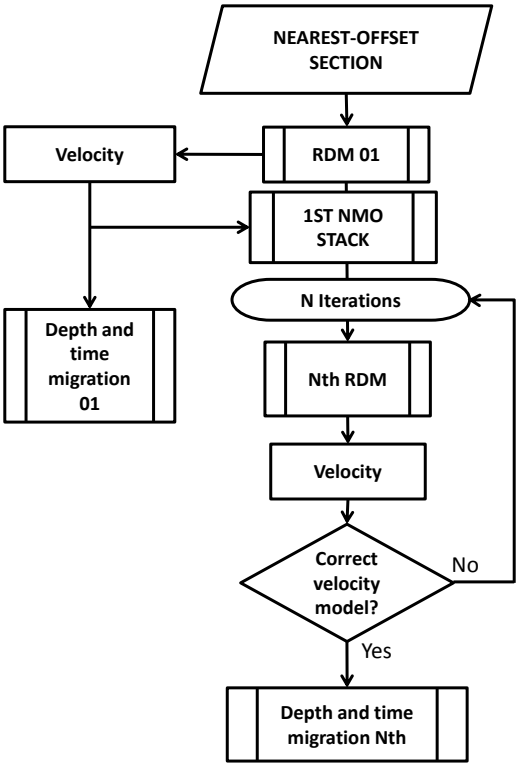


(b)

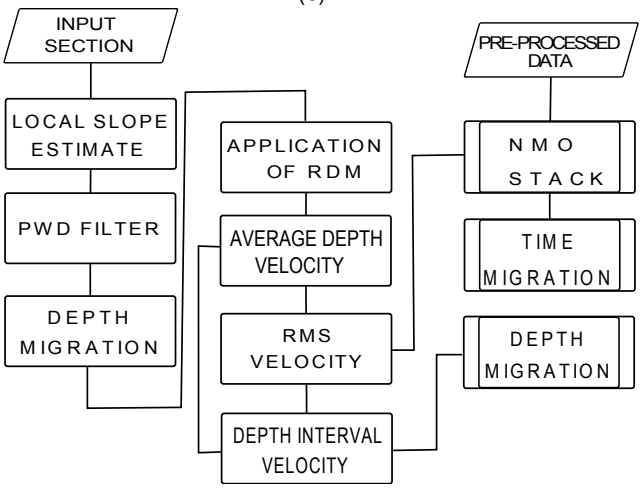


Figure 3: Processing flowcharts. (a) RDM processing sequence. (b) RDM velocity analysis.

**The Viking-Graben dataset**

In this work, we have applied our new RDM-based processing sequence to a real dataset from the Viking Graben in the North Sea Basin, provided by Exxon Mobil.

*Dataset description*

The cited Viking Graben dataset was acquired with 1001 shot points and 120 channels. The sampling rate was 4 ms and the total recording time was 6 s. The distance between the shot points and between the receivers was 25 m. The minimum and maximum offsets were 262 m and 3237 m, respectively. The water depth along the seismic line was a relatively constant 300 m. The data contain a large number of diffraction events, which makes them is particularly well suited for an application of the RDM method. In geological terms, the presence of many diffraction events in the data means that there are many faults and discontinuities in the subsurface.

*Preprocessing*

The pre-processing steps consisted of trace muting, bandpass filtering with a zero-phase (6-12-50-70 Hz) Ormsby filter, and spherical divergence corrections. Moreover, these data need preprocessing to eliminate the water-bottom multiples before applying our methodology. We applied predictive deconvolution with 320 ms operator length and 20 ms prediction operator. Also, we used deconvolution with white noise (S/N=0.1) and predictive deconvolution to improve the amplitude resolution.

For comparison, we performed a conventional processing of the Viking-Graben data to obtain a post-stack time and depth-migrated images and the corresponding velocity models. These serve as a benchmark to evaluate the quality of the corresponding results from RDM processing. As a reference image of the Viking Graben, we used the time-migrated image of Gislan and McMechan (2003).

As previously mentioned, an RDM velocity analysis uses the information contained in the residual moveout of incorrectly migrated diffractions to update the velocity model. According to the theory of Coimbra et al. (2013), the RDM method requires the diffractions to be located in the migrated depth domain. We can identify a number of undermigrated diffractions in the depth domain. To better visualize the diffractions we windowed the migrated image from 0.8 km to 2 km in depth and from 8 km to 22 km in horizontal distance. This depth section was the input to the RDM method. Figure 4 shows the post-stack time- and depth-migrated (Kirchhoff migration) sections with the conventional velocity model and the RDM velocity model. As can be noted, despite of the differences in the velocity models, the results are quite similar. The conventional image in Figure 4a presents more focused reflectors, but their local lateral variation are a little stronger, and the reflector elements below 2.2 s in the left part of the image are not visible at all. In contrast, the reflectors in the time migration with the RDM velocity (Figure 4b) are a little weaker but smoother, and the reflector elements in the bottom left corner start to become interpretable. With the velocity models in the depth domain from the RDM and conventional processing, we performed Kirchhoff depth migrations (Figure 5). The resulting images show little differences in the structures, except for the depth positioning of the reflectors. Though in the conventional image (Figure 5a), the reflectors again are slightly better focused, the RDM image (Figure 5b) shows an improved location of faults. This indicates that the velocity model found in the second iteration of the RDM processing is of acceptable quality.

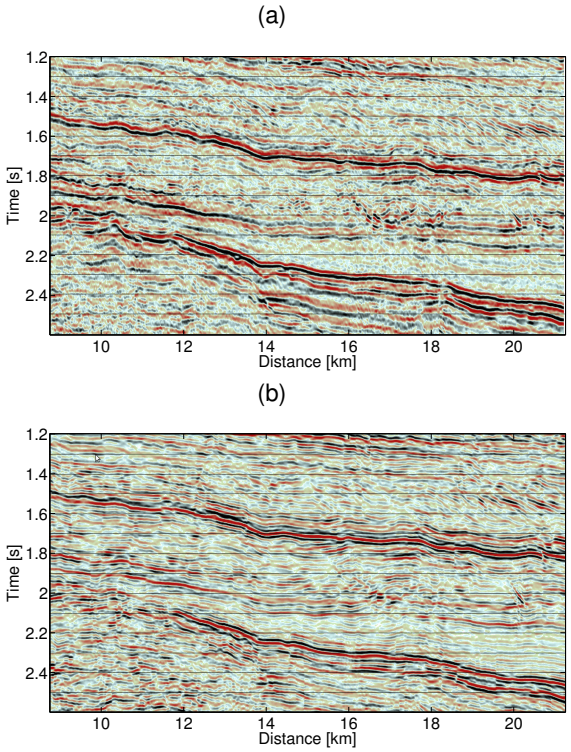


Figure 4: Time migrated sections with the model from (a) conventional processing and (b) RDM processing.

**Conclusions**

In this paper we have constructed a new processing flow for velocity analysis based on the residual-moveout analysis of incorrectly migrated diffraction events of Coimbra et al. (2013). A key element of our new processing sequence is the attenuation of reflected energy by means of plane-wave-destruction (PWD) filters. It is important to emphasize that we do not aim at suggesting that our methodology is better or worse than conventional methodologies. We are simply trying to point out that there are promising alternatives to conventional processing. Considering diffractions might help to extract additional information from the data which is not made use of in conventional processing.

With our workflow, it was possible in the case of a real Viking Graben dataset to construct an acceptable velocity model purely from diffraction information. In more complicated situations, a combination of diffraction and reflection information might still be superior to using reflections alone. While it is hard to quantify the seismic processing time, especially when the time depends on human interaction, our workflow has demonstrated that the information contained in diffraction events can be made accessible in a fraction of the time needed for conventional processing. Note that also in this aspect, the diffraction filtering was essential because a part of the processing

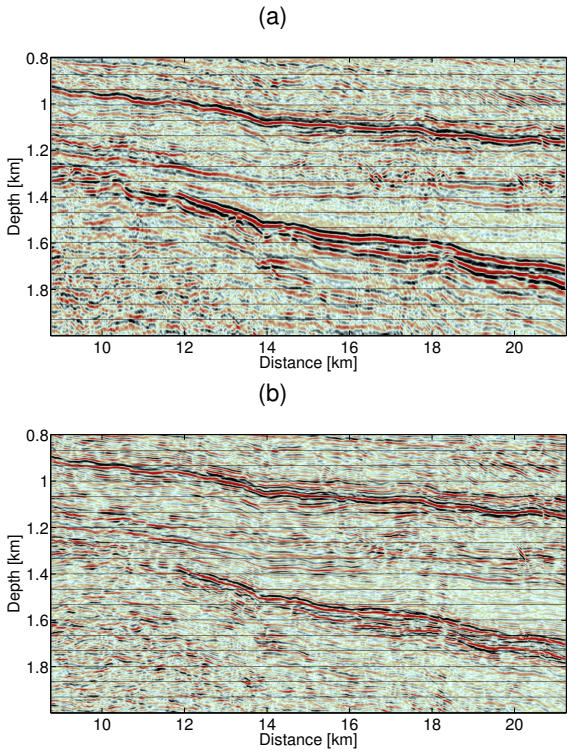


Figure 5: Depth-migrated sections with interval models from (a) conventional processing and (b) RDM processing.

time in our procedure is spent on the identification and interpretation of diffractions.

It is important to emphasize that we do not aim at suggesting that our methodology is better or worse than conventional methodologies. We are simply trying to point out that there are promising alternatives to conventional processing. Considering diffractions might help to extract additional information from the data which is not made use of in conventional processing. With our workflow, it was possible in the case of a real Viking Graben dataset to construct an acceptable velocity model purely from diffraction information. In more complicated situations, a combination of diffraction and reflection information might still be superior to using reflections alone.

**Acknowledgments**

The authors would like to thank the Exxon Mobil for providing the Viking Graben dataset and SMAART-JV for providing the Sigsbee2B data and model. This work was kindly supported by the Brazilian agencies CAPES, FINEP, and CNPq, as well as Petrobras and INCT-GP- Brazil.

**References**

Alonaizi, F., R. Pevzner, A. Bóna, M. Alshamry, E. Caspari, and B. Gurevich, 2014, Application of diffracted wave analysis to time-lapse seismic data for CO2 leakage detection: Geophysical Prospecting, **62**, 197–209.

Alonaizi, F., R. Pevzner, A. Bóna, V. Shulakova, and B. Gurevich, 2013, 3D diffraction imaging of linear features and its application to seismic monitoring: Geophysical Prospecting, **61**, 1206–1217.

Claerbout, J. F., 1992, Earth soundings analysis—processing versus inversion: Presented at the Blackwell Scientific Publications.

Coimbra, T. A., J. J. S. de Figueiredo, J. Schleicher, A. Novais, and J. C. Costa, 2013, Migration velocity analysis using residual diffraction moveout in the poststack depth domain: Geophysics, **78**, S125–S135.

de Figueiredo, J., F. Oliveira, E. Esmi, L. Freitas, J. Schleicher, A. Novais, P. Sussner, and S. Green, 2013, Automatic detection and imaging of diffraction points using pattern recognition: Geophysical Prospecting, **61**, 368–379.

Fomel, S., 2009, Applications of plane-wave destruction filters: Geophysics, **67**, 1946–1960.

Gislan, B. M., and G. A. McMechan, 2003, Processing, inversion, and interpretation of a 2D seismic data set from the north viking graben, north searocessing, inversion, and interpretation of a 2d seismic data set from processing, inversion and interpretation of a 2d sesimic data set from the north viking graben, north sea: Geophysics, **68**, 837–848.

Hale, D., 2007, Local dip filtering with directional laplacians: CWP Report, **567**.

Hubral, P., M. Tygel, and J. Schleicher, 1996, Seismic image waves: Geoph. J. Int., **125**, 431–442.

Khaidukov, V., E. Landa, and T. J. Moser, 2004, Diffraction imaging by focusing-defocusing: An outlook on seismic superresolution: Geophysics, **69**, 1478–1490.

Klokov, A., and S. Fomel, 2013, Separation and imaging of seismic diffractions using migrated dip-angle gathers: Geophysics, **77**, S131–S143.

Landa, E., and M. Reshef, 2009, Separation, imaging, and velocity analysis of seismic diffractions using migrated dip-angle gathers: 79th Ann. Internat. Meeting, SEG, Expanded Abstracts, 2176–2180.

Landa, E., V. Shtivelman, and B. Gelchinsky, 1987, A method for detection of diffracted waves on commom-offset sections.: Geophysical Prospecting, **35**, 359–374.

Liu, T., J. Hu, and H. Wang, 2013, Diffraction wavefield separation and imaging using singular spectrum analysis: Hola mundo, 78th EAGE Conference and Exhibition incorporating SPE EUROPEC, 10–13.

Novais, A., J. Costa, and J. Schleicher, 2008, GPR velocity determination by image-wave remigration: Journal of Applied Geophysics, **65**, 65–72.

Sava, P., B. Biondi, and J. Etgen, 2005, Wave-equation migration velocity analysis by focusing diffractions and reflections: Geophysics, **70**, U19–U27.

Schleicher, J., J. C. Costa, L. T. Santos, A. Novais, and M. Tygel, 2009, On the estimation of local slopes: Geophysics, **74**, 25–33.

Tsingas, C., B. E. Marhfoul, S. Satti, and A. Dajani, 2011, Diffraction imaging as an interpretation tool: First Break, **29**, 57–61.

Zhang, R., 2009, Imaging the earth using seismic diffractions.